

1           **Association of Human Mobility and Weather Conditions with Dengue Mosquito**  
2           **Abundance during the COVID-19 Pandemic in Hong Kong**

3  
4           Yufan Zheng<sup>a,b</sup>, Keqi Yue<sup>a,c</sup>, Eric W. M. Wong<sup>b</sup>, Hsiang-Yu Yuan<sup>a,d,\*</sup>

5  
6           <sup>a</sup>Department of Biomedical Sciences, Jockey Club College of Veterinary Medicine and Life  
7           Sciences, City University of Hong Kong, Hong Kong SAR, China

8           <sup>b</sup>Department of Electrical Engineering, College of Engineering, City University of Hong  
9           Kong, Hong Kong SAR, China

10           <sup>c</sup>Department of Chronic Disease Epidemiology, Yale School of Public Health, New Haven,  
11           CT, United States

12           <sup>d</sup>Centre for Applied One Health Research and Policy Advice, Jockey Club College of  
13           Veterinary Medicine and Life Sciences, City University of Hong Kong, Hong Kong SAR,  
14           China

15           \*Correspondence: sean.yuan@cityu.edu.hk

16

17 **ABSTRACT**

18 **Background**

19 While *Aedes* mosquitoes, the Dengue vectors, were expected to expand their spread due to  
20 international travel and climate change, the effects of human mobility and low rainfall  
21 conditions on them are largely unknown. We aimed to assess these influences during the  
22 COVID-19 pandemic in Hong Kong, characterized by varying levels of human mobility.

23

24 **Methods**

25 Google's human mobility indices (including residential, parks and workplaces) and weather  
26 conditions (total rainfall and mean temperature) together with *Aedes albopictus* abundance  
27 and extensiveness monitored using Gravidtrap were obtained between April 2020 and August  
28 2022. Distributed lag non-linear models with mixed-effects models were used to explore their  
29 influence in three areas in Hong Kong.

30

31 **Findings**

32 The relative risk (RR) of mosquito abundance was associated with low rainfall (<50 mm)  
33 after 4.5 months, with a maximum of 1.73, compared with 300 mm. Heavy rainfall (>500  
34 mm) within 3 months was also associated with a peak of RR at 1.41. Warm conditions (21-  
35 30°C; compared with 20°C) were associated with a higher RR of 1.47 after half a month.  
36 Residential mobility was negatively associated with mosquito abundance. The model  
37 projected that if residential mobility in the year 2022 was reduced to the level before the  
38 COVID-19 pandemic, the mosquito abundance would increase by an average of 80.49%  
39 compared to the actual observation.

40

41 **Significance**

42 Both the human mobility and the lag effect of meteorological factors can be critical for the  
43 prediction of vector dynamics, and stay-at-home policy may be useful for its control in  
44 certain regions.

45

46 **AUTHOR SUMMARY**

47 Previous studies have demonstrated that both meteorological factors and human mobility  
48 were linked to the risk of Dengue transmission, with rainfall potentially exerting delayed  
49 effects. Moreover, dry conditions have been found to increase Dengue risk in recent years.  
50 However, the impact of these factors on vector (mosquito) activity remains unclear. This  
51 study assessed the effect of human mobility and rainfall on the Dengue mosquito. The  
52 Gravitrap indices were used to characterize local mosquito (*Aedes Albopictus*) abundance and  
53 extensiveness conditions. We used established Gravitrap indices to characterize mosquito  
54 abundance and extensiveness in Hong Kong. We found that i) the decrease in residential  
55 mobility might increase mosquito abundance and extensiveness; and ii) low rainfall (<50 mm)  
56 was associated with a higher risk of mosquito abundance after 4.5 months. Additionally,  
57 heavy rainfall was associated with increased mosquito activity risk. The future mosquito  
58 activity risk is expected to increase because of the relaxation of social distancing measures  
59 after the COVID-19 pandemic along with climate change. The results suggest that non-linear  
60 delayed effects of meteorological factors together with human mobility change can be used  
61 for the Dengue mosquito forecast. Social distancing may be a way to reduce the risk of *Aedes*  
62 *albopictus*.

## 63 INTRODUCTION

64 Dengue fever (DF) is one of the most widespread mosquito-borne diseases, with an estimated  
65 390 million infections each year (1). *Aedes aegypti* and *Aedes albopictus* are two Dengue  
66 vectors. Global warming can facilitate their spread, leading to increasing risk in certain  
67 previously non-endemic subtropics, including southern China (2). In addition, according to a  
68 recent study, the risk of DF incidence can also be largely influenced by social distancing  
69 measures and human movement behaviours (3). Hong Kong, a metropolitan in southern  
70 China, faces an increased risk of Dengue outbreaks (4). Understanding how human mobility  
71 together with weather conditions affects *Aedes* mosquito abundance in Hong Kong helps  
72 make an early assessment of Dengue risk and decision-making in vector control.

73

74 In response to the increasing risk of DF (4), Hong Kong has established a Gravidtrap system  
75 for vector surveillance since 2020 to replace the Ovitrap. The Gravidtrap was developed to  
76 capture female *Aedes Albopictus* (5). In addition to the extensiveness (i.e. the distribution) of  
77 *Aedes Albopictus*, which could be measured by both traps, the new trap also monitored the  
78 abundance (i.e. the number) of mosquitoes.

79

80 During 2020 and 2022, social distancing was regularly introduced to reduce the spread of  
81 COVID-19. In 2022, strict social distancing was introduced during the COVID-19 Omicron  
82 wave. The strict social distancing might affect the likelihood of mosquitoes biting humans,  
83 especially *Aedes albopictus*, which tends to stay outside (6). Therefore, incorporating human  
84 mobility into mosquito prediction modelling is essential, especially when social distancing is  
85 implemented.

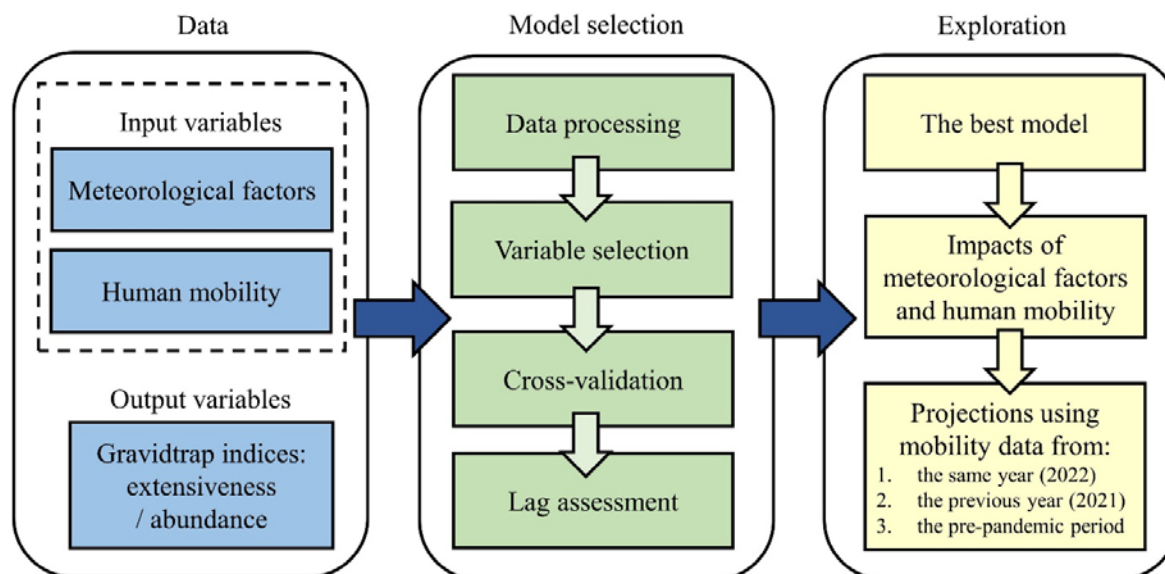
86

87 While a warm condition has a known impact on mosquito development, breeding, survival,  
88 etc., (7) the effects of rainfall are diverse, with both heavier and lower rainfall being  
89 associated with increased Dengue risk. Rainfall was an important Dengue risk factor (1,8),  
90 but recent studies found that drought conditions were also associated with a higher risk of  
91 Dengue incidence at long lead times of up to 5 months (9,10). Similarly, springtime rainfall, a  
92 few months before seasonal Dengue outbreaks, appeared to be negatively associated with  
93 annual Dengue incidence in Taiwan and Hong Kong (4,11). These previous studies suggested  
94 a varied relationship between hydroclimatic factors and Dengue incidence with delay effects  
95 (4,9–11). However, whether these delay effects occurred through influencing mosquito  
96 population dynamics remains largely unknown.

97

98 Our study aimed to assess the influence of human mobility on the abundance and  
99 extensiveness of *Aedes albopictus*, taking account of the nonlinear lagged effects of total  
100 rainfall and mean temperature (Figure 1). The results provided important insights for Dengue  
101 risk prediction and control.

102



103

104

105 **Figure 1 Schematic flow for exploration of different factors in the mosquito**  
 106 **extensiveness and abundance predictions.** WAIC was used for variable selection. The best  
 107 model was determined after the results were cross-validated and compared with different  
 108 lagged periods.

109

## 110 METHODS

### 111 Meteorological data

112 Meteorological data in Hong Kong were collected based on the weather stations in three  
 113 regions from the Hong Kong Observatory (12), including daily total rainfall and daily mean  
 114 temperature. We collected the data from April 2020 to August 2022 and divided it into three  
 115 areas (13): Hong Kong Island and Kowloon (HKK), New Territories East (NTE), and New  
 116 Territories West (NTW) (Table S1). Monthly total rainfall and monthly mean temperature (i.e.  
 117 obtained by averaging the daily mean temperatures) were calculated from these daily  
 118 measurements (Table S2). The meteorological factors for each area are the average value of  
 119 selected weather stations within that area (Supplementary Methods).

120

### 121 Human mobility data

122 Human mobility data for Hong Kong were collected from Google to represent the human  
 123 behavioural changes in response to the COVID-19 pandemic and social distance measures  
 124 during the study period (14). We used three categories of places in human mobility data,  
 125 including residential, parks and workplaces. All indices were computed relative to a baseline  
 126 day. The baseline day is the median value from the 5 weeks Jan 3–Feb 6, 2020. The monthly  
 127 human mobility index was calculated for model prediction (see Supplementary Methods).

128

### 129 Mosquito activity data

130 Mosquito activity data were provided by the Food and Environmental Hygiene Department  
 131 (15). Two indices were measured by the mosquito Gravidtrap surveillance: The Area Density  
 132 Index (ADI) defined as the number of mosquitoes captured in the traps (used to represent the  
 133 abundance of *Aedes albopictus*); and the Area Gravidtrap Index (AGI), defined as the  
 134 proportion of Gravidtraps that are found to have positive results in a specific area (used to  
 135 represent the extensiveness of *Aedes albopictus*).

136

137 We calculated the abundance and extensiveness for each area during each month  $t$ . First, the  
 138 index for each area (i.e. HKK, NTE, and NTW) was calculated as the average index for all  
 139 Gravidtrap sites in the region.

140

141 The average monthly mosquito extensiveness in area  $A$  is defined as:

142

$$143 \quad \overline{AGI}^A(t) = \sum_{m_i \in M^A(t)} (AGI^{m_i}(t)) / n_m^A(t) \quad (\text{eq. 1})$$

144

145 where  $n_m^A$  represents the total number of mosquito monitoring sites in area  $A$ .  $AGI^{m_i}$   
 146 represents the AGI in the surveyed area  $m_i$ .  $M^A = \{m_1, m_2, \dots, m_i\}$  is a collection of sites  
 147 (surveyed areas), in which  $m_i$  represents each site in the area.

148

149 The monthly abundance  $N^A(t)$  (per 1,000 traps) in area  $A$  is defined as:

150

$$151 \quad N^A(t) = \sum_{m_i \in M^A(t)} (AGI^{m_i}(t) \cdot ADI^{m_i}(t) \cdot 1000) / n_m^A(t) \quad (\text{eq. 2})$$

152

153 where  $ADI^{m_i}(t)$  represents the mean ADI at the site  $m_i$  in month  $t$ .

154

### 155 **Model development**

156 We developed prediction models for mosquito abundance and extensiveness based on  
 157 distributed-lagged non-linear models (DLNM) (16). For mosquito abundance prediction, we  
 158 assumed the mosquito number per 1000 traps follows the negative binomial distribution and  
 159 selected the log function as the link function. Let  $\lambda_t$  be the mosquito number per 1000 traps in  
 160 the month  $t$ , such as:

161

$$\lambda_t \sim NB(u_t, \kappa)$$

162

163 where  $u_t$  is distribution mean of  $\lambda_t$  at month  $t$  and  $\kappa$  is the overdispersion parameter in the  
 164 negative binomial distribution.  $\lambda_t$  in area,  $A$  can be measured by monthly mosquito  
 165 abundance  $N^A(t)$  (see eq. 2). Then, the regression model to predict mosquito abundance was:

166

$$167 \quad \log(\lambda_t) = \beta + \gamma + S + f.w(R_t, l_1) + f.w(T_t, l_2) + m_t + \alpha \quad (\text{eq. 3})$$

168

169 where  $f.w(R_t, l_1)$  and  $f.w(T_t, l_2)$  represent the nonlinear exposure-lag functions of total  
 170 rainfall  $R_t$  from 0 to  $l_1$  months and mean temperature  $T_t$  from 0 to  $l_2$  months in  $t^{th}$  month,  
 171 respectively;  $S$  is the area random effect;  $\gamma$  is the monthly random effect;  $\beta$  is the yearly  
 172 random effect;  $\alpha$  is the intercept; and  $m_t$  is the human mobility index in one category (e.g.  
 173 residential areas, workplaces, or parks) at  $t^{th}$  month.

174

175 In the mosquito extensiveness prediction, we assumed the number of positive traps follows  
 176 the binomial distribution and selected the logit function as the link function. Let  $Y_t$  be the  
 177 number of positive traps in the  $t^{th}$  month, following the binomial distribution with the total  
 178 number of the traps ( $n_t$ ), and the probability of a positive trap ( $p_t$ ) in the  $t^{th}$  month, such as:

179

$$Y_t \sim B(n_t, p_t)$$

180

181 where  $p_t$  at each surveyed area  $A$  can be measured by  $\overline{AGI}^A$  (see eq. 1).  $n_t$  can be calculated  
 182 as the product of the number of surveyed sites and the average number of traps per site. In  
 183 Hong Kong, an average of 55 Gravidtrap were placed in each selected site. Similarly, the  
 184 regression model to predict mosquito extensiveness was:

185

186

$$\text{logit}(p_t) = \beta + \gamma + S + f.w(R_t, l_1) + f.w(T_t, l_2) + m_t + \alpha \quad (\text{eq. 4})$$

187

### 188 **Model selection criteria**

189

190

191

192

193

194

195

196

197

198

199

200

201

### 201 **Comparison between mosquito abundance and extensiveness**

202

203

204

205

206

For comparing the predictive performance among mosquito abundance and extensiveness, we used two standardized mosquito indices to unify the scales of different indices: the standardized abundance index (SAI) and the standardized extensiveness index (SEI). The SAI was:

$$SAI = \lambda / \sigma_\lambda$$

207

208

209

210

where  $\lambda$  and  $\sigma_\lambda$  represent mosquito abundance and standard deviation of mosquito abundance, respectively. Similarly, the SEI was:

$$SEI = p / \sigma_p$$

211

212

213

where  $p$  and  $\sigma_p$  represent mosquito extensiveness and standard deviation of mosquito extensiveness, respectively.

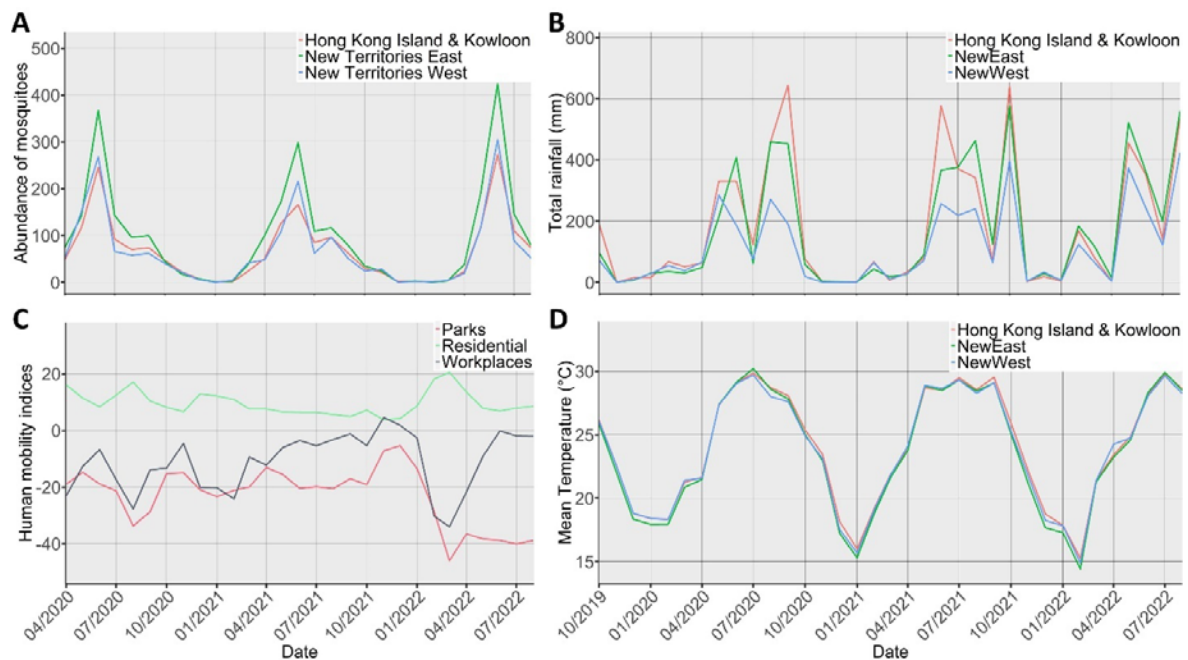
214 **RESULTS**215 **Data analysis**

216 In Hong Kong, mosquito abundance exhibited strong seasonal patterns, growing in the spring  
 217 (March-May), peaking in the early summer (June or July), and remaining nearly at 0 in the  
 218 winter (December-February) (Figure 2A). Among three predefined regions, NTE (a  
 219 northeastern region) recorded higher mosquito abundance (i.e. the number of *Aedes*  
 220 *albopictus*) than others. Mosquito extensiveness (i.e. the distribution of *Aedes albopictus*) had  
 221 a similar pattern of variation to abundance (Figure S1 and Figure S2). Two mosquito  
 222 standardized indices were proposed for mosquito abundance and extensiveness prediction  
 223 (Figure S3). in Hong Kong from April 2020 to August 2022. During the study period, human  
 224 mobility generally fluctuated at the beginning but showed rapid declines in parks and  
 225 workplaces and a sharp increase in residential since January 2022. This rapid change  
 226 reflected the behavioural changes and social distancing measures introduced during the  
 227 COVID-19 Omicron wave (Figure 2B).

228

229 The monthly total rainfall typically exceeded 300mm during summer and early autumn (June-  
 230 October) and was mostly less than that during winter and early spring (November-April) but  
 231 varied substantially between different regions and years. For example, in 2020–2021, HKK (a  
 232 southern region) had the most total rainfall, while NTW (a northwestern region) had the least  
 233 (Figure 2C). In 2022, all the regions experienced higher levels of total rainfall in February  
 234 than the previous year. The monthly mean temperature among these three regions was similar,  
 235 with the highest at about 30°C around July and the lowest at about 15°C in January or  
 236 February (Figure 2D).

237



238

239

240 **Figure 2 The monthly change in mosquito abundance and its predictors in Hong Kong.**

241 (A) Mosquito abundance; (B) Total rainfall; (C) Human mobility; (D) Mean temperature. In

242 A, B, and D, red refers to Hong Kong Island and Kowloon (HKK); blue refers to New

243 Territories East (NTE); and green refers to New Territories West (NTW).

244

245

246



247 **Model selection of mosquito abundance and extensiveness**

248 After initial variable selection, a baseline model for mosquito abundance prediction (Model A;  
249 see Table 1) was obtained. The candidate models in mosquito abundance prediction (see eq. 3)  
250 include Model A, Model A-M<sub>p</sub>, Model A-M<sub>w</sub>, and Model A-M<sub>r</sub>. After incorporating human  
251 mobility in residential, the best model for abundance (Model A-M<sub>r</sub>) was obtained using  
252 LOOCV. The best model for extensiveness (Model E-M<sub>r</sub>) also contained the same set of  
253 variables.

254

255 **Table 1 Comparison of candidate models for mosquito abundance.**

256 The top six rows represent the results of variable selection to obtain the best model. The  
257 bottom six rows represent the results of sensitivity analysis to ensure the best time lag of  
258 total rainfall and mean temperature. Model A comprised the total rainfall with lags from 0 to  
259 6 months, mean temperature with lags from 0 to 2 months, and random effects for years,  
260 months, and regions were used as a baseline model. Model A-M<sub>p</sub>, Model A-M<sub>w</sub>, and Model  
261 A-M<sub>r</sub> were models incorporating the human mobility index in parks, workplaces, and  
262 residential based on Model A, respectively.

Model	Model formula	WAIC	MSE in LOOCV
Model A1	$\beta + \gamma + S + \alpha$	741.12	—
Model A2	$\beta + \gamma + S + f. w(R_t, 6) + \alpha$	727.31	—
Model A	$\beta + \gamma + S + f. w(R_t, 6) + f. w(T_t, 2) + \alpha$	681.60	0.63
Model A-M <sub>p</sub>	$\beta + \gamma + S + f. w(R_t, 6) + f. w(T_t, 2) + m_p + \alpha$	677.92	0.65
Model A-M <sub>w</sub>	$\beta + \gamma + S + f. w(R_t, 6) + f. w(T_t, 2) + m_w + \alpha$	658.89	0.46
Model A-M <sub>r</sub>	$\beta + \gamma + S + f. w(R_t, 6) + f. w(T_t, 2) + m_r + \alpha$	<b>651.87</b>	<b>0.37</b>
Model A-M <sub>r</sub> 1	$\beta + \gamma + S + f. w(R_t, 5) + f. w(T_t, 2) + m_r + \alpha$	666.57	—
Model A-M <sub>r</sub> 2	$\beta + \gamma + S + f. w(R_t, 4) + f. w(T_t, 2) + m_r + \alpha$	668.37	—
Model A-M <sub>r</sub> 3	$\beta + \gamma + S + f. w(R_t, 3) + f. w(T_t, 2) + m_r + \alpha$	664.26	—
Model A-M <sub>r</sub> 4	$\beta + \gamma + S + f. w(R_t, 2) + f. w(T_t, 2) + m_r + \alpha$	671.56	—
Model A-M <sub>r</sub> 5	$\beta + \gamma + S + f. w(R_t, 1) + f. w(T_t, 2) + m_r + \alpha$	669.79	—
Model A-M <sub>r</sub> 6	$\beta + \gamma + S + f. w(R_t, 6) + f. w(T_t, 1) + m_r + \alpha$	653.22	—

263

264

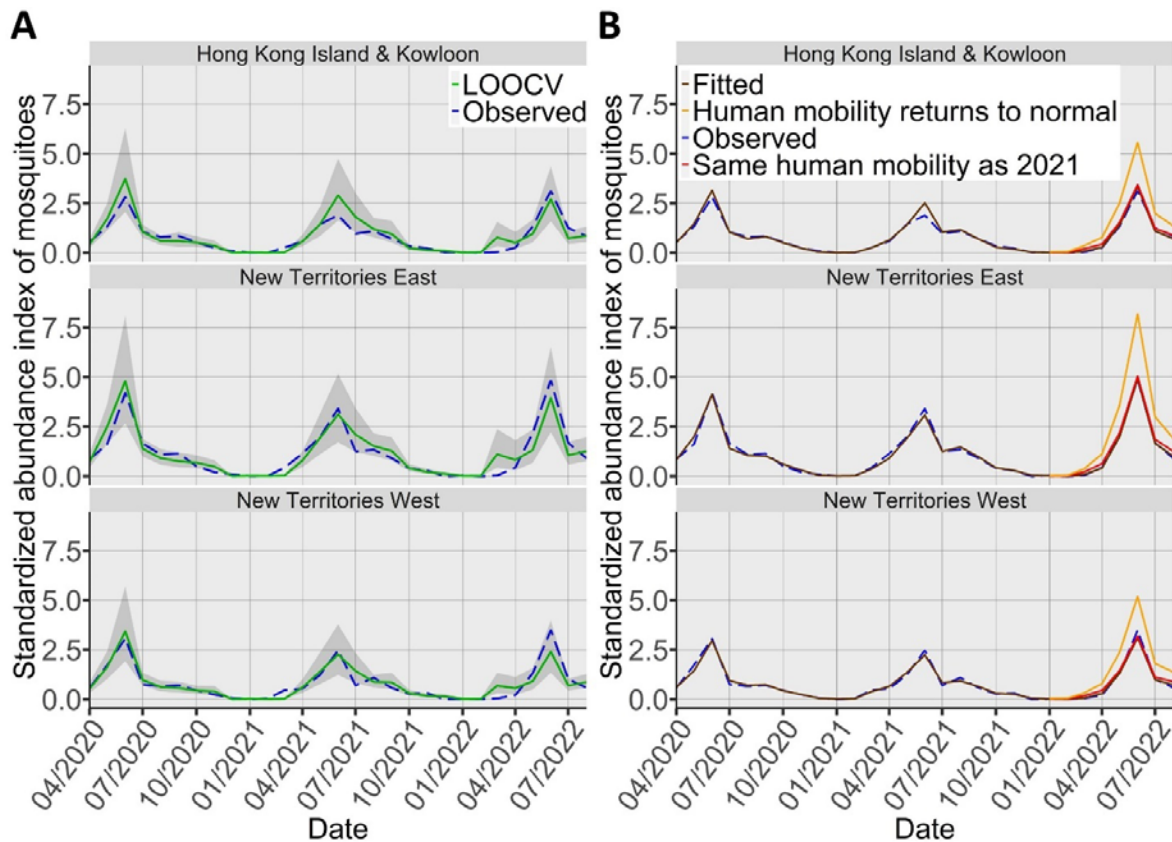
265 **Prediction of mosquito activity using weather and human mobility**

266 Overall, both models A-M<sub>r</sub> and E-M<sub>r</sub> showed similar predictive performances (Table 1 and  
267 Table S4), The model fit for mosquito abundance appeared to be slightly better than that for  
268 mosquito extensiveness as more observed data points in the year 2022 were within 95%  
269 confidence interval (CI) of the predicted values for mosquito abundance (Figure 3A and  
270 Figure S4A). It might be because mosquito abundance is more weather-related while  
271 mosquito extensiveness is more related to the presence of potential breeding places or the  
272 placement of the traps (Table 1 and Table S4).

273

274 The model estimated that residential mobility change has a negative effect on the mosquito  
275 abundance prediction (correlation coefficient = -0.075 (95%CI, -0.118--0.033); see Table S5).  
276 On the other hand, park mobility and workplace mobility had a positive effect on mosquito  
277 abundance. The effects of the human mobility indices on mosquito extensiveness were  
278 consistent with mosquito abundance.

279



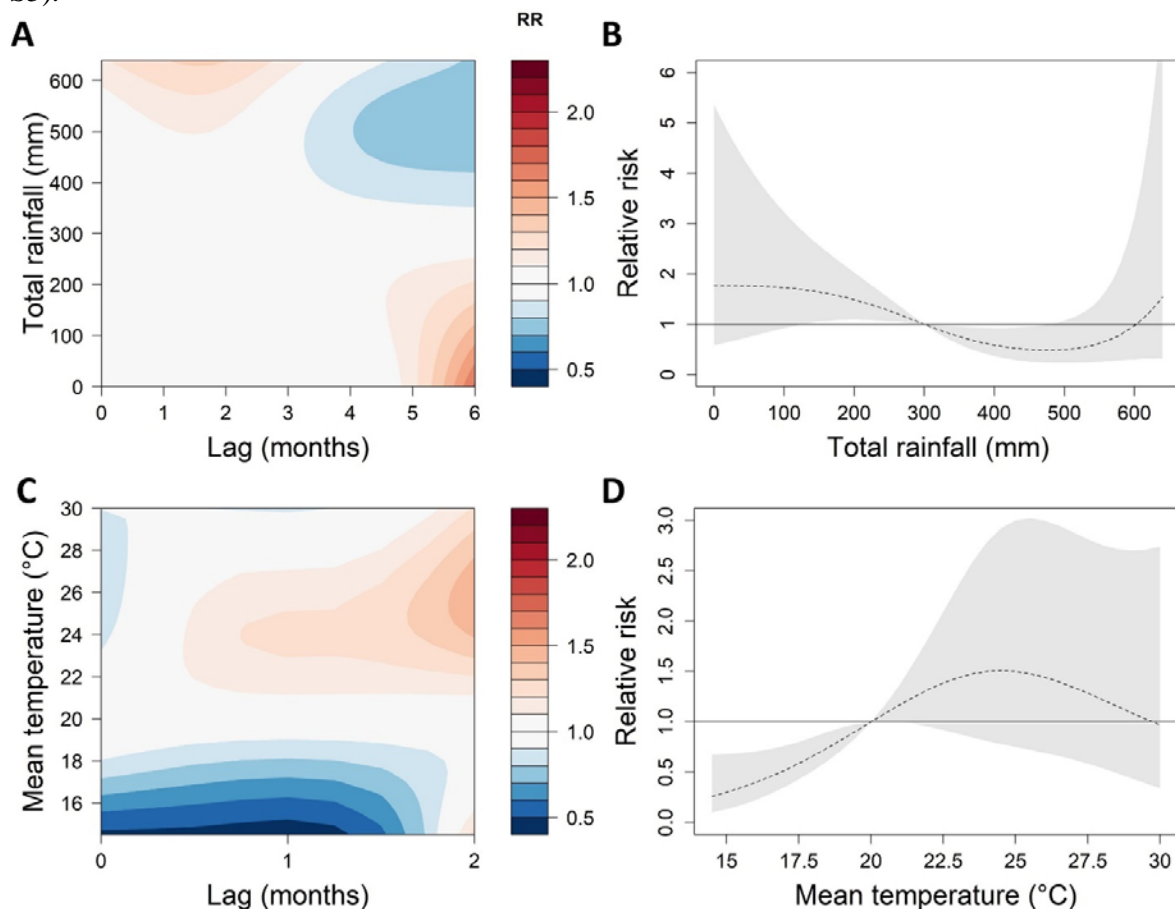
280  
281  
282 **Figure 3 Comparison of observed and predicted results using the best model for**  
283 **mosquito abundance.** (A) Predicted results of mosquito abundance using leave-one-out  
284 cross-validation (LOOCV) with Model A-M<sub>r</sub>. The grey shaded area represents the 95%  
285 confidence interval. The blue dashed line represents observed data and the green solid line is  
286 the leave-one-out cross-validation result. (B) Projected results of mosquito abundance in the  
287 year 2022 under different scenarios in human mobility (residential category): human mobility  
288 returns to the COVID-19 pre-pandemic period (orange) and the same human mobility as year  
289 2021 (red). The blue dashed line represents observed data and the brown solid line represents  
290 fitted data.

### 291 292 **Effects of weather conditions**

293 Higher relative risks in mosquito abundance were observed in the conditions of extremely  
294 low (<50 mm) or heavy rainfall (>500 mm) (Figure 4A). Compared with the reference (300  
295 mm), a reduction in total rainfall was associated with a higher relative risk (RR) after about  
296 4.5 months, reaching a maximum of 1.73 (95%CI, 1.19-2.51). However, heavy rainfall  
297 conditions (>500 mm) were associated with a higher RR within 3 months, reaching a  
298 maximum of 1.31 (95%CI, 0.99-1.73). When lagged effects were accumulated, the maximum  
299 RR occurred at no rainfall (Figure 4B). The accumulated RR decreased with total rainfall up  
300 to about 500 mm but increased again thereafter.

301  
302 Compared with the reference mean temperature (20 °C), the warm conditions (21-30 °C) were  
303 associated with an increased risk of mosquito abundance after about half a month, leading to  
304 a maximum RR of 1.47 (95%CI, 0.94-2.32) at 25.5 °C (Figure 4C). When lagged effects were  
305 accumulated, the RR increased with mean temperatures from 15 °C to 26 °C but decreased at  
306 warmer conditions (>26 °C) (Figure 4D). The associations between total rainfall and mean

307 temperature with mosquito extensiveness were similar to that of mosquito abundance (Figure  
308 S5).



309  
310

311 **Figure 4 Effects of total rainfall and mean temperature on mosquito abundance using**  
312 **the best model.** (A) Relative risk (RR) by total rainfall and lag months; (B) Cumulative RR  
313 for total rainfall; (C) RR by mean temperature and lag months; (D) Cumulative RR for mean  
314 temperature. The reference of total rainfall and mean temperature are 300mm and 20°C,  
315 respectively. The deeper the shade of red, the greater the increase in RR compared with the  
316 reference. The deeper the shade of blue, the greater the decrease in RR compared with the  
317 reference. The black dashed line represents the cumulative exposure-response association.  
318 The grey shaded area represents the 95% confidence interval.

319

### 320 **Model projections for human mobility change**

321 The model projected the mosquito abundance in two alternative scenarios for the year 2022: 1)  
322 same residential mobility as before the COVID-19 Omicron wave, indicating returning to a  
323 normal state, and 2) same residential mobility as year 2021, indicating a weak social  
324 distancing. In the first scenario when human mobility returned to normal (before the COVID-  
325 19 pandemic), cumulative mosquito abundance in all areas significantly increased by an  
326 average of 80.49% compared to the actual situation. The cumulative mosquito abundance in  
327 the HKK is increasing the most, at 83.41%. In the second scenario, cumulative mosquito  
328 abundance in all areas was only slightly higher than the actual situation by an average of  
329 10.96% (Figure 3B). The projection results of mosquito extensiveness were similar to those  
330 of mosquito abundance (Figure S4B).

331

### 332 **Sensitivity analysis**

333 Prediction models in mosquito abundance and extensiveness were sensitive in the variable  
334 selection of the lag of total rainfall, the lag of mean temperature, and the human mobility  
335 indices (Table 1 and Table S4). Model A, the WAIC decreased from 681.60 to 651.88 after  
336 adding the residential mobility index. When the total rainfall lag reduced from 6 months to  
337 other lengths, WAIC increased. Similarly, When the mean temperature lag reduced from 2  
338 months to 1 month, WAIC increased. The durations of lags in total rainfall and mean  
339 temperature that produced the lowest WAIC for mosquito abundance and extensiveness were  
340 selected.  
341

## 342 **DISCUSSION**

### 343 **Influence of human mobility on mosquito activity**

344 Understanding the association between human mobility and mosquito activity helps in  
345 forecasting the risk of DF transmission and developing effective strategies for its prevention.  
346 Our results showed that residential mobility was negatively associated with mosquito  
347 abundance, while mobility indices in parks and workplaces showed positive associations. The  
348 results can be explained by that the increase in outdoor activities provides more chances to  
349 feed meals (blood) to *Aedes albopictus* (6). The model projected that if human mobility (i.e.  
350 residential) returned to normal in 2022, the risk of mosquito activity would increase  
351 significantly (80% more) during the peak. In addition to border reopening (18), a possible  
352 increase in mosquito abundance, extensiveness, and DF incidence might appear due to more  
353 outdoor human activity.

354  
355 Recently, Brady et al. also reported that Dengue incidence was associated with certain  
356 Google human mobility indices (e.g. workplace mobility and park mobility) during the  
357 COVID-19 period (3). The difference between their modelling results with our study may be  
358 explained by some factors. The impact of human mobility may be different in mosquito  
359 activity and Dengue incidence. Moreover, an increase in residential mobility may have  
360 different impacts on mosquitoes between *Aedes Albopictus* and *Aedes Aegypti*, which are  
361 both the main vectors to transmit DF. However, *Aedes Albopictus* was the only mosquito  
362 vector found in Hong Kong. Those differences suggest that prevention of DF through vector  
363 control should take into account the impact of human mobility on mosquito and Dengue  
364 incidence simultaneously.

### 365 **Impact of total rainfall lags and mean temperature on mosquito activity**

366 Rainfall appeared to influence mosquito activity by different mechanisms. Both dry and wet  
367 conditions were found to be associated with an increased risk of Dengue infection in China  
368 (19). We found that heavy rainfall conditions (>500 mm) within 3 months were associated  
369 with a higher risk of *Aedes* mosquito activity. On the other hand, low rainfall (<50 mm) was  
370 associated with a higher risk with a longer lag (Figure 4A). A possible explanation is that  
371 early low rainfall (around late winter or springtime) helps to maintain the number of  
372 mosquito eggs or larval sites without the flushing effect (20). *Aedes albopictus* survives the  
373 winter at its egg stage. When more rain comes in a warmer environment after a period of dry  
374 conditions, there will be a large number of eggs hatching simultaneously leading to a bloom  
375 in adult mosquitoes. This scenario can be particularly important when the mosquito begins to  
376 grow, corresponding to the period from springtime to the pre-rainy season before the  
377 monsoon in many subtropical regions in Asia (21). The results suggest that, in southern China  
378 or its neighbourhoods, some extreme hydroclimatic events, such as delayed monsoon or  
379 drought conditions, during springtime might increase the Dengue risk in summertime. Severe  
380 drought conditions have been observed in spring in 2018 in Hong Kong, and 2015 and 2023  
381 in Taiwan, followed by significant outbreaks (11,22,23).

382  
383  
384 In our findings, the mean temperature was positively associated with mosquito activity until  
385 exceeding a threshold. We observed an increased mosquito activity risk after about a half-  
386 month, similar to the time that *Aedes albopictus* may use to develop from eggs to adults. A  
387 maximum level occurred about two months later when the mean temperature was between  
388 25 and 26°C (Figure 4C). Our findings in Hong Kong were consistent with the previous  
389 studies using Dengue incidence (9).

### 390 **Implications**

392 The spread of vector-borne diseases such as DF, Malaria, and Zika diseases can have serious  
393 consequences for human health and even lead to large-scale deaths. Residential mobility  
394 indicates the change in the time people spend at home, as the outcome of social distancing  
395 measures during the COVID-19 pandemic period. Therefore, our results suggest that social  
396 distancing measures may be an important intervention to reduce mosquito abundance.  
397 Furthermore, our results indicate that knowing the impact of hydroclimatic events on these  
398 diseases can provide important risk projections for the future. In vector control of South-East  
399 Asia, the Global Vector Control Response prioritized enhancing vector surveillance,  
400 forecasting, and monitoring effects of different factors (24). Extreme weather or  
401 hydroclimatic events, such as heavy rains or droughts are happening more frequently in the  
402 world (25). They might have critical influences on the dynamics of the mosquito population  
403 depending on the time of their occurrences (26). Incorporating extreme hydroclimatic events  
404 (such as drought conditions) together with human mobility patterns helps to forecast Dengue  
405 risk and inform public health decisions in vector control for its prevention.

406

#### 407 **Limitations and future works**

408 Several limitations exist within this study. The mosquito activity may also be influenced by  
409 other human-induced factors, such as land use type and urbanization process (27,28). Control  
410 measures may have been taken specifically around those Gravidtrap sites. But during the  
411 zero-COVID period in Hong Kong, the impact of these mosquito control measures was  
412 expected to be smaller. Furthermore, extreme weather events can affect a variety of climatic  
413 factors, some of which might be important factors for mosquito activity, such as typhoons  
414 (29). We chose two important weather factors according to the previous studies (1,8), instead  
415 of considering all of them. Recent studies have assessed the impact of climate change on  
416 Dengue risk (19,30). Incorporating the insights from our findings can provide a better  
417 understanding of how extreme weather conditions and human mobility might influence the  
418 Dengue vector's abundance and control.

419

#### 420 **Conclusion**

421 As the COVID-19 pandemic ends and borders reopen, the risk of DF is expected to be higher  
422 in many parts of the world. The study found that social distancing measures were associated  
423 with reduced mosquito abundance and extensiveness. Furthermore, low rainfall was  
424 associated with a higher risk of mosquito activity (abundance and extensiveness) with the 4.5  
425 months lag (Figure 4A), which was able to explain the recent findings of the delayed effects  
426 of weather conditions on Dengue incidence (9,10). The results suggested that the highest  
427 Dengue risk after drought conditions was likely to be affected by the spread of Dengue  
428 mosquitoes.

429

#### 430 **Contributors**

431 YZ, KY and HY designed the study. YZ and KY developed the methods, performed the  
432 research, and accessed and verified the data. YZ and KY wrote the initial draft of this  
433 manuscript. YZ and HY contributed to the interpretation of the results. YZ, HY, and EW  
434 helped revise the manuscript. All authors had full access to all the data in the study and had  
435 final responsibility for the decision to submit for publication.

436

#### 437 **Acknowledgements**

438 We thank Ming Wai Lee from the Food and Environmental Hygiene Department, the Govern  
439 ment of HKSAR.

440

## REFERENCES

- 441 1. Bhatt S, Gething PW, Brady OJ, Messina JP, Farlow AW, Moyes CL, et al. The global distribution and  
442 burden of dengue. *Nature*. 2013;496(7446):504–507.
- 443 2. Liu B, Gao X, Ma J, Jiao Z, Xiao J, Hayat MA, et al. Modeling the present and future distribution of  
444 arbovirus vectors *Aedes aegypti* and *Aedes albopictus* under climate change scenarios in Mainland  
445 China. *Science of the Total Environment*. 2019;664:203–214.
- 446 3. Chen Y, Li N, Lourenço J, Wang L, Cazelles B, Dong L, et al. Measuring the effects of COVID-19-  
447 related disruption on dengue transmission in southeast Asia and Latin America: a statistical modelling  
448 study. *The Lancet infectious diseases*. 2022;22(5):657–667.
- 449 4. Yuan HY, Liang J, Lin PS, Sucipto K, Tsegaye MM, Wen TH, et al. The effects of seasonal climate  
450 variability on dengue annual incidence in Hong Kong: A modelling study. *Scientific Reports*.  
451 2020;10(1):4297.
- 452 5. Lee C, Vythilingam I, Chong CS, Razak MAA, Tan CH, Liew C, et al. Gravitrap for management of  
453 dengue clusters in Singapore. *American Journal of Tropical Medicine and Hygiene*. 2013;88(5):888–  
454 892.
- 455 6. Bonizzoni M, Gasperi G, Chen X, James AA. The invasive mosquito species *Aedes albopictus*: Current  
456 knowledge and future perspectives. *Trends in Parasitology*. 2013;29(9):460–468.
- 457 7. Reinhold JM, Lazzari CR, Lahondère C. Effects of the environmental temperature on *Aedes aegypti* and  
458 *Aedes albopictus* mosquitoes: A review. *Insects*. 2018;9(4):158.
- 459 8. World Health Organization. Dengue and severe dengue. 2023. Available at [https://www.who.int/news-  
460 room/fact-sheets/detail/dengue-and-severe-dengue](https://www.who.int/news-room/fact-sheets/detail/dengue-and-severe-dengue). (Accessed 17 March 2023)
- 461 9. Lowe R, Lee SA, Brady OJ, Bastos L, Colón-González FJ, on Climate Change C, et al. Combined  
462 effects of hydrometeorological hazards and urbanisation on dengue risk in Brazil: a spatiotemporal  
463 modelling study. *Lancet Planet Health*. 2021;5(4):e209–e219.
- 464 10. Lowe R, Gasparrini A, Van Meerbeek CJ, Lippi CA, Mahon R, Trotman AR, et al. Nonlinear and  
465 delayed impacts of climate on dengue risk in Barbados: A modelling study. *PLoS Medicine*.  
466 2018;15(7):e1002613.
- 467 11. Yuan HY, Wen TH, Kung YH, Tsou HH, Chen CH, Chen LW, et al. Prediction of annual dengue  
468 incidence by hydro-climatic extremes for southern Taiwan. *International Journal of Biometeorology*.  
469 2019;63:259–268.
- 470 12. Hong Kong Observatory. Climatological Information Services. Available at:  
471 <https://www.hko.gov.hk/en/cis/climat.htm>. (Accessed 3 Jan 2024)
- 472 13. The Government of the Hong Kong Special Administrative Region. Summary of the Geographical  
473 Constituencies. 2016. Available at <https://www.elections.gov.hk/legco2016/eng/maps.html>. (Accessed 3  
474 Jan 2024)
- 475 14. Google. Community Mobility Reports. Available at <https://www.google.com/covid19/mobility/>.  
476 (Accessed 3 Jan 2024)
- 477 15. Food and Environmental Hygiene Department. Vector-borne diseases. Available at  
478 [https://www.fehd.gov.hk/english/pestcontrol/dengue\\_fever/index.html](https://www.fehd.gov.hk/english/pestcontrol/dengue_fever/index.html). (Accessed 3 Jan 2024)
- 479 16. Gasparrinia A, Armstrong B, Kenward MG. Distributed lag non-linear models. *Statistics in Medicine*.  
480 2010;29(21):2224–2234.
- 481 17. Vehtari A, Gelman A, Gabry J. Practical Bayesian model evaluation using leave-one-out cross-  
482 validation and WAIC. *Stat Comput*. 2017;27:1413–1432.
- 483 18. Chen Y, Li N, Lourenço J, Wang L, Cazelles B, Dong L, et al. Measuring the effects of COVID-19-  
484 related disruption on dengue transmission in southeast Asia and Latin America: a statistical modelling  
485 study. *Lancet Infectious Diseases*. 2022;22(5):657–667.
- 486 19. Li C, Liu Z, Li W, Lin Y, Hou L, Niu S, et al. Projecting future risk of dengue related to  
487 hydrometeorological conditions in mainland China under climate change scenarios: a modelling study.  
488 *Lancet Planetary Health*. 2023;7(5):e397–406.
- 489 20. Seidahmed OME, Eltahir EAB. A Sequence of Flushing and Drying of Breeding Habitats of *Aedes*  
490 *aegypti* (L.) Prior to the Low Dengue Season in Singapore. *PLoS Neglected Tropical Diseases*.  
491 2016;10(7):e0004842.
- 492 21. Zhao S, Bei N, Sun J. Mesoscale analysis of a heavy rainfall event over Hong Kong during a pre-rainy  
493 season in South China. *Advances in Atmospheric Sciences*. 2007;24:555–572.
- 494 22. Hong Kong Observatory. The Year's Weather-2018. 2019. Available at  
495 <https://www.hko.gov.hk/en/wxinfo/pastwx/2018/ywx2018.htm>. (Accessed 3 Jan 2024)
- 496 23. Brendan Wong. Radio Taiwan International. Taiwan potentially facing worst drought in 30 years. 2023.  
497 Available at <https://en.rti.org.tw/news/view/id/2009076>. (Accessed 3 Jan 2024)
- 498 24. Control of Neglected Tropical Diseases GMPHIEVC and R. Global vector control response: progress in  
499 planning and implementation. 2020. Available at  
500 <https://www.who.int/publications/i/item/9789240007987>. (Accessed 3 Jan 2024)
- 501

- 502 25. Fischer EM, Sippel S, Knutti R. Increasing probability of record-shattering climate extremes. *Nature*  
503 *Climate Change*. 2021;11(8):689–695.
- 504 26. Liyanage P, Tozan Y, Overgaard HJ, Aravinda Tissera H, Rocklöv J. Effect of El Niño–Southern  
505 Oscillation and local weather on *Aedes* vector activity from 2010 to 2018 in Kalutara district, Sri  
506 Lanka: a two-stage hierarchical analysis. *Lancet Planetary Health*. 2022;6(7):e577–585.
- 507 27. Lee JM, Wasserman RJ, Gan JY, Wilson RF, Rahman S, Yek SH. Human activities attract harmful  
508 mosquitoes in a tropical urban landscape. *Ecohealth*. 2020;17:52–63.
- 509 28. Yin S, Hua J, Ren C, Wang R, Weemaels AI, Guénard B, Shi Y, Lee T, Yuan H, Chong KC, Tian L.  
510 Spatial pattern assessment of dengue fever risk in subtropical urban environments: The case of Hong  
511 Kong. *Landscape and Urban Planning*. 2023;237:104815
- 512 29. Kao B, Lin CH, Wen TH. Measuring the effects of typhoon trajectories on dengue outbreaks in tropical  
513 regions of Taiwan: 1998–2019. *International Journal of Biometeorology*. 2023;67:1311–1322.
- 514 30. Gibb R, Colón-González FJ, Lan PT, Huong PT, Nam VS, Duoc VT, et al. Interactions between climate  
515 change, urban infrastructure and mobility are driving dengue emergence in Vietnam. *Nature*  
516 *Communications*. 2023;14(1):8179.

517